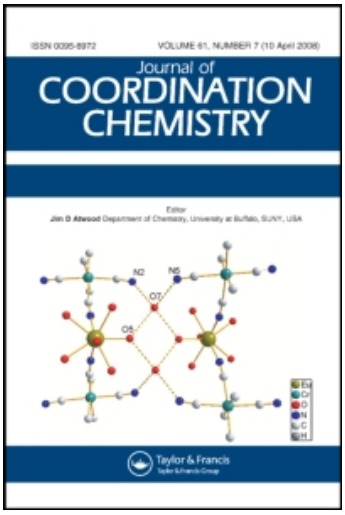

Journal of Coordination Chemistry
Publication details, including instructions for authors and subscription information:
http://www.informaworld.com/smpp/title~content=t713455674

Synthesis, crystal structure, and DNA-binding of a 3-D netlike supramolecular manganese picrate complex with 2,6-bis(benzimidazol-2-yl)pyridine

Zhen-Zhong Yan[a]; Zhi-Hong Xu[b]; Guo-Liang Dai[a]; Hua-Ding Liang[a]; Song-Lin Zhao[a]
[a] Department of Pharmaceutics and Chemical Engineering, Taizhou University, Linhai 317000, PR China [b] College of Chemistry and Chemical Engineering, Xuchang University, Xuchang 461000, PR China

First published on: 25 March 2010

To cite this Article Yan, Zhen-Zhong , Xu, Zhi-Hong , Dai, Guo-Liang , Liang, Hua-Ding and Zhao, Song-Lin(2010) 'Synthesis, crystal structure, and DNA-binding of a 3-D netlike supramolecular manganese picrate complex with 2,6-bis(benzimidazol-2-yl)pyridine', Journal of Coordination Chemistry, 63: 7, 1097 — 1106, First published on: 25 March 2010 (iFirst)
To link to this Article: DOI: 10.1080/00958971003728288
URL: http://dx.doi.org/10.1080/00958971003728288

Journal of Coordination Chemistry
Vol. 63, No. 7, 10 April 2010, 1097–1106

Taylor & Francis
Taylor & Francis Group

Synthesis, crystal structure, and DNA-binding of a 3-D netlike supramolecular manganese picrate complex with 2,6-bis(benzimidazol-2-yl)pyridine

ZHEN-ZHONG YAN*†, ZHI-HONG XU‡, GUO-LIANG DAI†, HUA-DING LIANG† and SONG-LIN ZHAO†

†Department of Pharmaceutics and Chemical Engineering, Taizhou University, Linhai 317000, PR China
‡College of Chemistry and Chemical Engineering, Xuchang University, Xuchang 461000, PR China

(*Received 26 June 2009; in final form 17 November 2009*)

Manganese picrate with 2,6-bis(benzimidazol-2-yl)pyridine (L) has been prepared and characterized by elemental analysis, IR spectroscopy, and single-crystal X-ray diffraction. The complex crystallizes in the triclinic system, space group *P–1* with $a = 14.234(3)$ Å, $b = 14.324(2)$ Å, $c = 15.242(2)$ Å, $\alpha = 77.569(2)^\circ$, $\beta = 63.350(3)^\circ$, $\gamma = 82.130(2)^\circ$, and $Z = 2$. Interaction of the complex with calf-thymus DNA (CT-DNA) has been investigated with diverse spectroscopic techniques and viscosity measurements, and the binding constant is $1.76 \times 10^5\,\mathrm{mol}^{-1}$. Results suggest that the complex bind to CT-DNA *via* intercalation.

Keywords: Crystal structure; 2,6-Bis(benzimidazol-2-yl)pyridine; Manganese picrate complex; DNA-binding

1. Introduction

Considerable attention has been given to the synthesis of bis-benzimidazole compounds because of their properties in cancer therapy. Various studies with bis-benzimidazole derivatives have shown that their binding affinity to calf-thymus DNA (CT-DNA) correlates positively with the *in vitro* topoisomerase inhibitory potency or cytotoxicity [1]. The chelation of 2,6-bis(benzimidazol-2-yl)pyridine (L) is depicted in scheme 1 [2–4]. Metal complexes having polypyridyl moieties have been extensively studied as DNA structural probes and DNA-dependent electron transfer probes [5–7]. Interaction of metal complexes with DNA has been examined due to their cationic character, water solubility, stability in water, and spectroscopic signature. Bünzli *et al.* [8–11] have reported that attachment of five-membered rings to the central pyridine in extended tridentate ligand (L) improves affinity for metal ions. Some metal complexes of polypyridine ligands activate endonucleolytic cleavage in DNA in the presence

*Corresponding author. Email: yanzhzh@tzc.edu.cn

Journal of Coordination Chemistry
ISSN 0095-8972 print/ISSN 1029-0389 online
DOI: 10.1080/00958971003728288

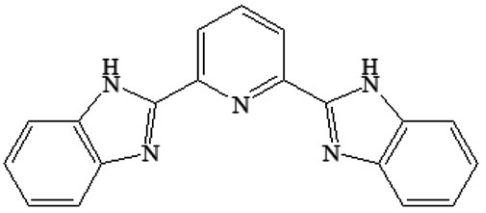

Scheme 1. The structure of L.

of external agents or footprinting agents and as models for the reactivity of some antitumor antibiotics [12].

In this work, an organic picrate possessing relatively weak coordination activity was chosen as a counter anion for manganese complex with 2,6-bis(benzimidazol-2-yl)-pyridine (L). Elemental analyses indicate a 1 : 2 : 2 : 1 metal-to-L-to-picrate-to-ethanol stoichiometry, $MnL_2(Pic)_2(C_2H_6O)$. The crystal structure indicates that $[MnL_2](Pic)_2$ link to each other by intermolecular hydrogen bonds and π–π stacking interactions to form a three-dimensional (3-D) netlike supermolecule. The interactions of DNA with the complex have been investigated to evaluate biological activity.

2. Experimental

2.1. *Materials and methods*

All reagents and solvents were purchased commercially and used without purification unless otherwise noted. $Mn(Pic)_2$ was prepared by the reaction of manganese carbonate and picric acid in hot water. Calf-thymus DNA (CT-DNA) was obtained from Sigma Chemicals Co. (USA) and used as received. The solutions of CT-DNA in 50 mmol NaCl, 5 mmol Tris-HCl (tris(hydroxymethyl) aminomethane hydrochloride) (pH 7.2) gave a ratio of UV-Vis absorbance of 1.8–1.9 : 1 at 260 and 280 nm, indicating that the DNA was sufficiently free of protein [13]. The concentration of DNA was determined spectrophotometrically using a molar absorptivity of 6600 $mol^{-1}\,cm^{-1}$ (260 nm) [14]. Doubly distilled water was used to prepare buffers.

Carbon, nitrogen, and hydrogen analyses were determined using an Elementar Vario EL. The IR spectra were recorded on a Nicolet 360 FT-IR instrument using KBr discs from 4000–400 cm^{-1}. The ^1H NMR spectrum was measured on a Varian Mercury-300B spectrometer in $CDCl_3$ solution with TMS as internal standard. The luminescence and phosphorescence spectra were obtained on a Hitachi RF-4500 spectrophotometer at room temperature.

2.1.1. Preparation of L. The ligand 2,6-bis(benzimidazol-2-yl)pyridine was prepared by reaction of pyridine-2,6-dicarboxylic acid and *O*-phenylenediamine in syrupy phosphoric acid (40 mL) at *ca* 230° for 4 h as described previously [15], yield 55%, m.p. > 250° (Found: C, 70.86; H, 4.05; N, 22.06. Calcd for L (%): C, 70.27; H, 4.03; N, 21.40). IR(cm^{-1}) in KBr pellet: ν(C=N) 1459s; ν(C=C): 1436s; ν(C–N):1274s;

ν(N–H) 3083 m, 3058 m and ν(O–H) 3180 m. ^{1}H NMR ($CDCl_3$, 300 MHz): 7.3–8.5 (m, aromatic), 13.2 (s, imino).

2.1.2. Synthesis of the manganese picrate complex. The manganese picrate complex was prepared as yellow powder by the reaction of $Mn(Pic)_2$ and L at 1 : 1 molar ratio in ethanol (Found: C, 52.47; H, 2.802; N, 19.47. Calcd for $MnL_2(Pic)_2(C_2H_6O)$ (%): C, 52.93; H, 3.08; N, 18.99). IR(cm^{-1}, KBr): ν(C=N): 1610; ν(C=C): 1441; ν(C–N): 1274; ν_{as}(–NO_2): 1555; ν_s(–NO_2): 1342.

2.2. *DNA-binding experiments*

Absorption titration experiments were performed by maintaining the metal complex concentration as constant at 10 μmol while varying the concentration of CT-DNA within 0.5–10 μmol. While measuring absorption spectra, equal quantity of CT-DNA was added to both the complex and the reference solution to eliminate the absorbance of DNA itself.

For fluorescence measurements, fixed amounts (10 μmol) of the complex were titrated with increasing amounts (0–50 μmol) of CT-DNA. The excitation wavelength was 415 nm, scan speed = 240 nm min^{-1}, and slit width 2.5/2.5 nm.

Viscosity experiments were conducted on an Ubbelohde viscometer immersed in a thermostatted water bath maintained at 25 ± 0.1°C. The data were presented as $(\eta/\eta_0)^{1/3}$ *versus* the ratio of the concentration of the compound to CT-DNA, where η is the viscosity of CT-DNA in the presence of the compound and η_0 is the viscosity of CT-DNA alone. The viscosity values were calculated from the observed flow time of CT-DNA containing solutions corrected from the flow time of buffer alone (t_0), $\eta = t - t_0$ [16].

2.3. *Crystal structure determination*

Yellow crystals suitable for X-ray diffraction were obtained by slow evaporation of the ethanol solution of the Mn complex. Single-crystal X-ray diffraction was performed on a Bruker SMART CCD diffractometer equipped with a graphite crystal monochromator situated in the incident beam for data collection. A single crystal with dimensions $0.30 \times 0.19 \times 0.17\,mm^3$ was chosen for X-ray diffraction studies. The determination of unit cell parameters and data collection were performed with Mo-Kα radiation ($\lambda = 0.71073$ Å) at 298(2) K on a Bruker SMART diffractometer. The structure was solved by direct methods using SHELXS program of the SHELXL-97 package and refined with SHELXL [17]. Manganese centers were located from the *E*-map and other non-hydrogen atoms were located in successive difference Fourier syntheses. The final refinement was performed by full matrix least squares with anisotropic thermal parameters for non-hydrogen atoms on F^2. The hydrogens were added geometrically and not refined. The final $R = 0.0885$ and $wR = 0.2046$ $(w = 1/[\sigma^2(F_o^2) + (0.0477P)^2 + 0.1617P]$, where $P = (F_o^2 + 2F_c^2)/3)$, $S = 1.001$, $(\Delta\rho)_{max} = 0.794$, $(\Delta\rho)_{min} = -0.417\,e\,Å^{-3}$, and $(\Delta/\sigma)_{max} = 0.000$.

3. Results and discussion

3.1. *Crystal structure of the title complex*

A summary of crystallographic data and details of the structure refinements are listed in table 1; selected bond lengths and angles are given in table 2.

As shown in figure 1, in $MnL_2(Pic)_2(C_2H_6O)$, Mn(II) is coordinated with six nitrogens from two tridentate L in a distorted octahedron. Two picrates are counter anions and one ethanol is in the outer coordination sphere. All atoms of the same L are almost in a plane, and the dihedral angle between two planes is 80.50°.

A 3-D netlike supramolecule (figure 2) was further formed through hydrogen bonds and π–π interactions. The π–π interactions between the picrate groups, which are formed between two benzene rings of the benzimidazole rings [the centroid (C14, C15, C16, C17, C18, and C19) to centroid distances are 3.800 Å (symmetry code: $1-x$, $1-y$, $1-z$); the centroid (C33, C34, C35, C36, C37, and C38) to centroid (C26, C33, C34, N9, and N10) distances are 3.909 Å (symmetry code: $1-x$, $-y$, $1-z$)] form a 2-D layer supramolecule [18]. In addition, the layers are linked by π–π interactions between two picrate ions [the centroid (C39, C40, C41, C42, C43, and C44) to centroid distances are 4.004 Å (symmetry code: x, y, z)] and intermolecular N–H $\cdots$ O and C–H $\cdots$ O hydrogen bonds between nitrogens of L and picrate. All of the relevant hydrogen-bonding values and symmetry codes are listed in table 3.

Table 1. Crystal and experimental data.

Empirical formula	$C_{52}H_{36}N_{16}O_{15}Mn$
Formula weight	1179.91
Temperature (K)	298(2)
Wavelength (Å)	0.71073
Crystal system	Triclinic
Unit cell dimensions (Å, °)	
a	14.234(3)
b	14.324(2)
c	15.242(2)
α	77.569(2)
β	63.350(3)
γ	82.130(2)
Volume (Å^3), Z	2709.5(8), 2
Calculated density (mg m^{-3})	1.446
Absorption coefficient (mm^{-1})	0.328
F(000)	1210
Crystal size (mm^3)	$0.30 \times 0.19 \times 0.17$
θ range for data collection (°)	2.12–25.01
Limiting indices	$-8 \le h \le 16$; $-17 \le k \le 17$; $-17 \le l \le 18$
Reflections collected	13,771
Independent reflection	9136 [R(int) = 0.0618]
Completeness to $\theta = 25.00$ (%)	95.8
Absorption correction	Semi-empirical from equivalents
Max. and min. transmission	0.9464 and 0.9080
Data/restraints/parameters	9136/451/835
Goodness-of-fit on F^2	1.001
Final R indices [$I > 2\sigma(I)$]	$R_1 = 0.0885$, $wR_2 = 0.2046$
R indices (all data)	$R_1 = 0.2379$, $wR_2 = 0.2985$
Largest difference peak and hole (e Å^{-3})	0.794 and 0.079
Refinement method	Full-matrix least-squares on F^2

3.2. *Absorption titration*

The electronic absorption spectroscopy in DNA-binding studies is one of the most useful techniques [19, 20]; absorption spectra of the complex in the absence and presence of CT-DNA (at a constant concentration of the complex) are given in figure 3. In the presence of DNA, absorption bands of the complex at 333 nm exhibit hypochromism of about 26.1% and bathochromism of about 13 nm. These spectral characteristics suggest that the complex interacts with DNA most likely through a mode that involves a stacking interaction between the aromatic chromophore and the base pairs of DNA.

Table 2. Selected bond lengths (Å) and angles (°).

Mn(1)–N(1)	2.228(7)	N(1)–Mn(1)–N(2)	72.0(3)
Mn(1)–N(6)	2.238(7)	N(1)–Mn(1)–N(4)	71.6(2)
Mn(1)–N(2)	2.253(7)	N(1)–Mn(1)–N(6)	162.4(3)
Mn(1)–N(7)	2.261(7)	N(1)–Mn(1)–N(7)	123.7(2)
Mn(1)–N(4)	2.262(7)	N(1)–Mn(1)–N(9)	93.2(3)
Mn(1)–N(9)	2.307(7)	N(2)–Mn(1)–N(4)	142.2(3)
		N(2)–Mn(1)–N(6)	118.6(2)
		N(2)–Mn(1)–N(7)	91.6(2)
		N(2)–Mn(1)–N(9)	99.3(2)
		N(4)–Mn(1)–N(6)	99.2(2)
		N(4)–Mn(1)–N(7)	100.4(2)
		N(4)–Mn(1)–N(9)	92.4(2)
		N(6)–Mn(1)–N(7)	71.9(3)
		N(6)–Mn(1)–N(9)	71.8(3)
		N(7)–Mn(1)–N(9)	143.0(3)

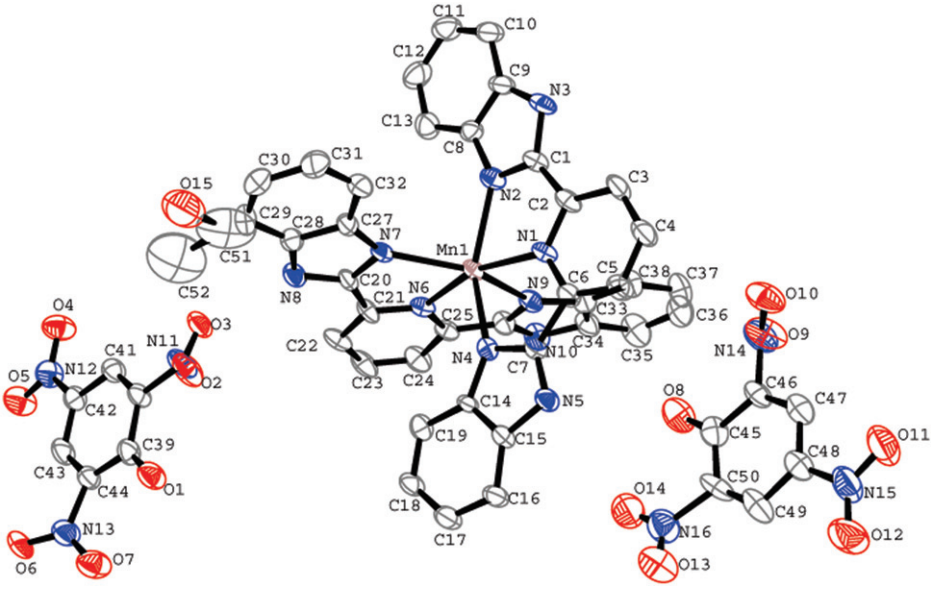

Figure 1. ORTEP diagram (30% probability ellipsoids) showing the molecular structure of the Mn complex (the free ethanol is omitted for clarity).

The absorption data were analyzed to evaluate the intrinsic binding constant K_b, which can be determined from [16]:

$$[DNA]/(\varepsilon_a - \varepsilon_f) = [DNA]/(\varepsilon_b - \varepsilon_f) + 1/K_b(\varepsilon_b - \varepsilon_f)$$

where [DNA] is the concentration of DNA in base pairs, the apparent absorption coefficient ε_a, ε_f, and ε_b correspond to $A_{obsd}/[M]$, the extinction coefficient of the free compound and the extinction coefficient of the compound when fully bound to DNA, respectively. In plots of $[DNA]/(\varepsilon_a - \varepsilon_f)$ *versus* [DNA], K_b is given by the ratio of slope to the intercept. The intrinsic binding constant K_b of the complex was $1.76 \times 10^5\,mol^{-1}$.

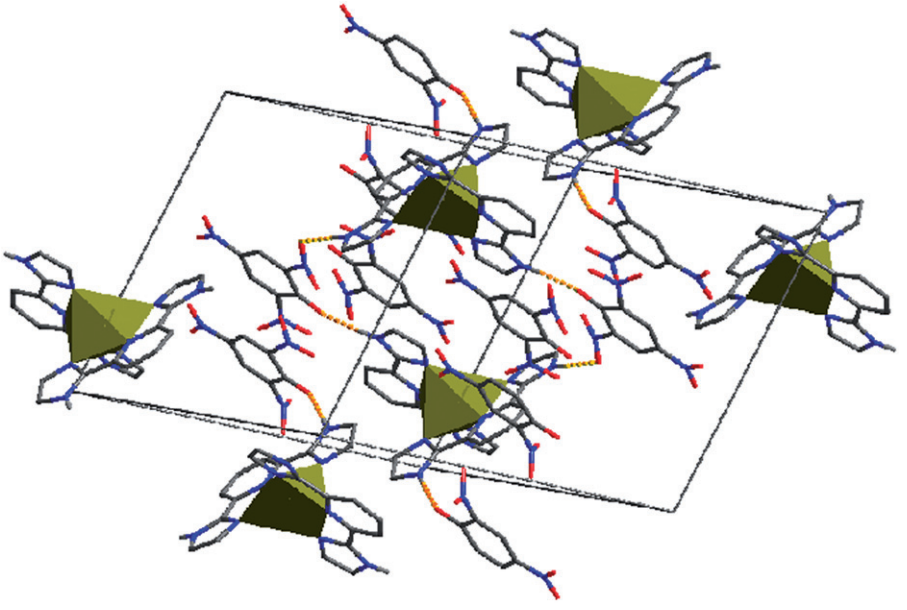

Figure 2. 3-D netlike supermolecule generated by intermolecular hydrogen bonds and π–π interactions in the title complex (hydrogen bonds are indicated by the yellow dashed lines).

Table 3. Hydrogen bonds in crystal packing (Å, °).

D–H···A	*d*(D–H)	*d*(H···A)	*d*(D···A)	∠DHA	Symmetry
N(3)–H(3)···O(15)	0.86	1.90	2.7452	168	$-1+x, y, 1+z$
N(5)–H(5)···O(1)	0.86	2.17	2.9981	160	
N(8)–H(8)···O(3)	0.86	2.08	2.9369	178	$1-x, 1-y, 1-z$
N(10)–H(10)···O(8)	0.86	1.90	2.7545	171	$1-x, -y, 1-z$
C(5)–H(5A)···O(1)	0.93	2.28	3.1621	159	
C(16)–H(16)···O(2)	0.93	2.36	3.1517	142	
C(23)–H(23)···O(10)	0.93	2.41	3.3393	174	$1+x, y, z$
C(24)–H(24)···O(9)	0.93	2.43	3.2123	142	$1-x, -y, 1-z$

3.3. *Thermal denaturation study*

DNA melting is observed when double-stranded DNA molecules are heated and separate into single strands; it occurs due to the disruption in intermolecular forces such as π stacking and hydrogen-bonding interactions between DNA base pairs. Here, a DNA melting experiment revealed that T_m of CT-DNA was 67 ± 0.2 and $74 \pm 0.2^{\circ}C$ in the absence and presence of the complex, respectively. However, for the ligand alone, there is no change in DNA melting temperature. The ΔT_m of $7^{\circ}C$ indicates that the binding cannot be classical intercalative. Such ΔT_m is generally associated with partial intercalation binding of the metal complex [21]. One would expect a much larger increase in T_m for classical intercalators [22–24]. A small ΔT_m also indicates weak binding of the complex to DNA. The change in T_m is indicative of moderate binding of the complex with DNA.

3.4. *Fluorescence study*

In the absence of DNA, the complex emits fluorescence in Tris buffer at room temperature, with a maximum at 415 nm (the excitation and emission slit widths were 2.5 nm). Upon addition of CT-DNA, emission intensities of the complex are quenched steadily (figure 4), implying that the complex interacts with DNA with photoelectron transfer from DNA to the complex [25–28]; the hydrophobic environment inside the DNA helix reduces the accessibility of water to the complex and complex mobility is restricted at the binding site, leading to the decrease of the vibrational modes of relaxation.

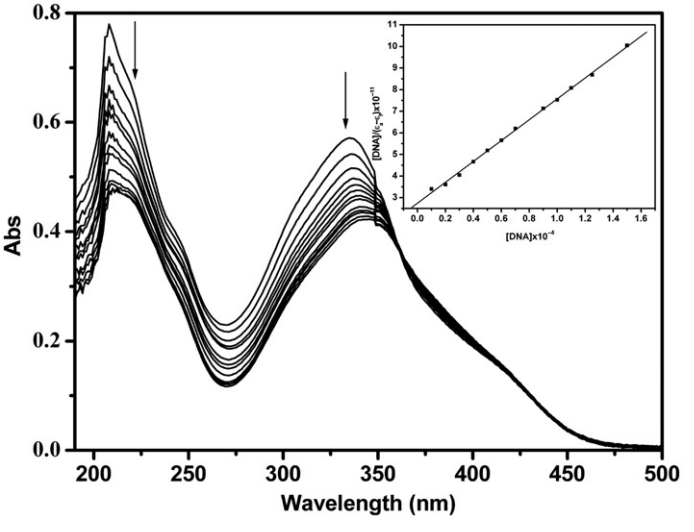

Figure 3. Electronic spectra of the complex ($10\,\mu mol\,L^{-1}$) in the presence of 0, 1, 2, 4, 6, 8, 10, 12, 14, 16, 18, 20, 22, 25, and $30\,\mu L$ $1.0 \times 10^{-3}\,mol\,L^{-1}$ CT-DNA. Arrow shows the absorbance changes upon increasing CT-DNA concentration. Inset shows the plots of $[DNA]/(\varepsilon_a - \varepsilon_f)$ *vs.* [DNA] for interaction between DNA and the complex.

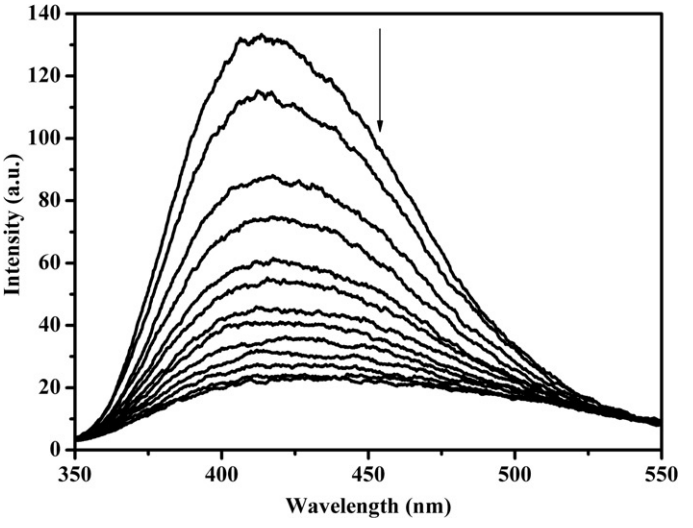

Figure 4. The fluorescence emission spectra of the complex upon increasing CT-DNA concentration at room temperature, concentration of the complex 1.0×10^{-3} mol L^{-1}.

3.5. *Viscosity measurements*

Spectroscopic experiments provide necessary, but not sufficient clues to support a binding mode. The measurements of DNA viscosity sensitive to DNA length are regarded as the least ambiguous and the most critical tests of binding in solution in the absence of crystallographic structural data [29]. A classical intercalation mode results in lengthening the DNA helix as base pairs are separated to accommodate the binding ligand, leading to the increase of DNA viscosity. In contrast, a partial nonclassical intercalation of ligand could bend (or kink) the DNA helix and reduce its effective length [30]. Upon addition of the complex, the viscosity of rod-like CT-DNA increased significantly, as illustrated in figure 5, which suggests that the complex binds to DNA by intercalation.

4. Conclusions

A manganese(II) complex with symmetrical tridentate ligand (L) was synthesized and characterized by elemental analysis, IR spectroscopy, and single-crystal X-ray diffraction. $[MnL_2](Pic)_2 \cdot C_2H_5OH$ are linked by intermolecular hydrogen bonds and π–π interactions to form a 3-D netlike supermolecule. Sun *et al.* [31] reported intrinsic binding constants K_b of 4.1×10^4 mol^{-1}. DNA binding of our complex was investigated by spectroscopic techniques and viscosity measurements, with intrinsic binding constants K_b of 1.76×10^5 mol^{-1}. The studies of metal complexes can give some guidance to explore the possible new drugs, but further studies will be needed to understand the selectivity of complexes.

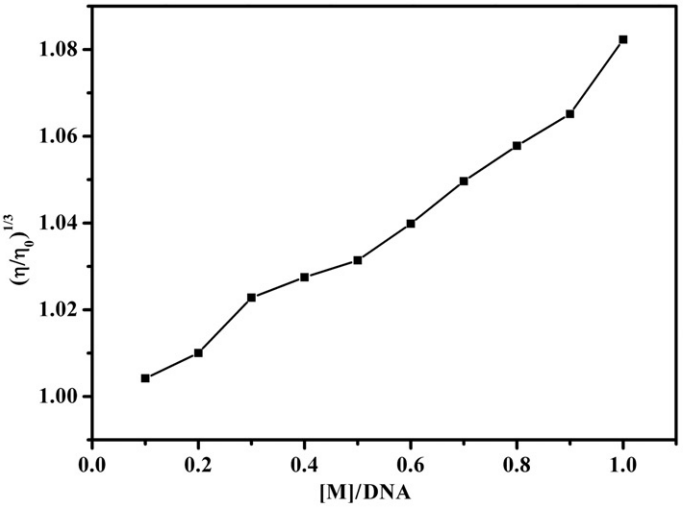

Figure 5. Effect of increasing amounts of the complexes on the relative viscosity of DNA at 25 ± 0.1°C.

Supplementary material

The X-ray crystallographic file, in CIF format, has been deposited with the Cambridge Crystallographic Data Center, CCDC No. 625773. Copy of this information may be obtained free of charge from the Cambridge Crystallographic Data Center, 12 Union Road, Cambridge, CB2 1EZ, UK (Email: deposit@ccdc.cam.ac.uk).

References

[1] P.R. Turner, W.A. Denny. *Mutant. Res.*, **355**, 141 (1996).
[2] Z.Z. Yan, Y. Tang, M.Y. Tan, W.S. Liu, D.Q. Wang. *Acta Chim. Sinica*, **65**, 607 (2007).
[3] G. Muller, J.C.G. Bunzli, K.J. Schenk, C. Piguet, G. Hopfgartner. *Inorg. Chem.*, **40**, 2642 (2001).
[4] F. Benetollo, G. Bombieri, K.K. Fonda, A. Polo, J.R. Quagliano, L.M. Vallarino. *Inorg. Chem.*, **30**, 1345 (1991).
[5] K.E. Erkkila, D.T. Odom, J.K. Barton. *Chem. Rev.*, **99**, 2777 (1999).
[6] C. Metcalfe, J.A. Thomas. *Chem. Soc. Rev.*, **32**, 215 (2003).
[7] I. Haq, P. Lincoln, D. Suh, B. Norden, B.Z. Choedhry, J.B. Chaires. *J. Am. Chem. Soc.*, **117**, 4788 (1995).
[8] C. Piguet, A.F. Williams, G. Bernardinelli, E. Moret, J.C.G. Bünzli. *Chim. Acta*, **75**, 1697 (1992).
[9] S. Petoud, J.C.G. Bünzli, K.J. Schenk, C. Piguet. *Inorg. Chem.*, **36**, 1345 (1997).
[10] H. Nozary, C. Piguet, P. Tissot, G. Bernardinelli, J.C.G. Bünzli, R. Deschenaux, D. Guillon. *J. Am. Chem. Soc.*, **120**, 12274 (1998).
[11] H. Nozary, C. Piguet, J.P. Rivera, P. Tissot, G. Bernardinelli, N. Vulliermet, J. Weber, J.C.G. Bünzli. *Inorg. Chem.*, **39**, 5286 (2000).
[12] X.H. Zou, B.H. Ye, H. Li, Q.L. Zhang, H. Chao, J.G. Liu, L.N. Ji. *J. Biol. Inorg. Chem.*, **6**, 143 (2001).
[13] S. Satyanarayana, J.C. Dabrowiak, J.B. Chaires. *Biochemistry*, **32**, 2573 (1993).
[14] J. Marmur. *J. Mol. Biol.*, **3**, 208 (1961).
[15] M.T. Caster, M. Rodriguez, A.J. Bard. *J. Am. Chem. Soc.*, **111**, 8901 (1989).
[16] S. Satyanarayana, J.C. Dabrowiak, J.B. Chaires. *Biochemistry*, **32**, 2573 (1993).
[17] G.M. Sheldrick. *SHELXS-97, A Program for X-ray Crystal Structure Solution, and SHELXL-97, A Program for X-ray Structure Refinement*, Gottingen University, Germany (1997).
[18] C. Janiak. *J. Chem. Soc., Dalton Trans.*, 3885 (2000).
[19] G.A. Jeffrey, H. Maluszynska, J. Mitra. *Int. J. Biol. Macromol.*, **7**, 336 (1985).

[20] A. Wolf, G.H. Shimer Jr, T. Meehan. *Biochemistry*, **26**, 6392 (1987).
[21] S. Arounaguiri, B.G. Maiya. *Inorg. Chem.*, **35**, 4267 (1996).
[22] M. Cory, D.D. McKee, J. Kagan, D.W. Henry, J.A. Miller. *J. Am. Chem. Soc.*, **107**, 2528 (1985).
[23] J.M. Kelly, A.B. Tossi, D.J. McConnell, C. OhUigin. *Nucleic Acids Res.*, **13**, 6017 (1985).
[24] G.A. Neyhart, N. Grover, S.R. Smith, W.A. Kalsbeck, T.A. Fairley, M. Cory, H.H. Thorp. *J. Am. Chem. Soc.*, **115**, 4423 (1993).
[25] J.M. Kelly, D.J. McConnell, C. OhUigin, A.B. Tossi, A.K. Mesmaeker, A. Masschelein, J. Nasielski. *J. Chem. Soc., Chem. Commun.*, 1821 (1987).
[26] V.G. Vaidyanathan, B.U. Nair. *J. Inorg. Biochem.*, **94**, 121 (2003).
[27] A. Kirsch-De Mesmaeker, G. Orellana, J.K. Barton, N.J. Turro. *Photochem. Photobiol.*, **52**, 461 (1990).
[28] P.X. Xi, X.H. Liu, H.L. Lu, Z.Z. Zeng. *Transition Met. Chem.*, **32**, 757 (2007).
[29] D.S. Pilch, M.J. Waring, J.S. Sun, M. Rougee, C.H. Nguyen, E. Bisagni, T. Garestier, C. Helene. *J. Mol. Biol.*, **232**, 926 (1993).
[30] D.S. Sigman, A. Mazumder, D.M. Perrin. *Chem. Rev.*, **93**, 2295 (1993).
[31] W. Sun, M. Jiang, Y.T. Li, Z.Y. Wu, W.B. Peng. *J. Coord. Chem.*, **62**, 2520 (2009).